Enhancing the Coherence Time of a Neutral Atom by an Optical Quartic Trap

Haobo Chang[1,2], Zhuangzhuang Tian[1,2], Xin Lv[1,2], Mengna Yang[1,2], Zhihui Wang[1,2], Qi Guo[1,2,3], Pengfei Yang[1,2], Pengfei Zhang[1,2], Gang Li[1,2*], and Tiancai Zhang[1,2*]

[1]*State Key Laboratory of Quantum Optics Technologies and Devices, Institute of Opto-Electronics, Shanxi University, Taiyuan 030006, China*
[2]*Collaborative Innovation Center of Extreme Optics, Shanxi University, Taiyuan 030006, China*
[3]*College of Physics and Electronic Engineering, Shanxi University, Taiyuan 030006, China*

(Received 9 May 2025; accepted manuscript online 29 September 2025)

The coherence time of an optically trapped neutral atom is a crucial parameter for quantum technologies. We found that optical dipole traps with higher-order spatial forms inherently offer lower decoherence rates compared to those with lower-order spatial forms. We formulated the decoherence rate caused by the variance of the differential energy shift and photon jumping rate. Then, we constructed blue-detuned harmonic and quartic optical dipole traps, and experimentally investigated the coherence time of a trapped single cesium atom. Specifically, we demonstrated a significant improvement in the coherence time of a single atom by employing a quartic trap with the same characteristic trap potential and size as its harmonic counterpart—achieving an enhancement from 315 ms to 474 ms. The experimental results qualitatively verified our theory. Our approach provides a novel method to enhance the coherence time of optically trapped neutral atoms.

DOI: 10.1088/0256-307X/42/11/110303 CSTR: 32039.14.0256-307X.42.11.110303

1. Introduction. As one of the basic parameters for quantum technologies, a long coherence time is always a stringent requirement.[1,2] In the context of optically trapped neutral atoms, research on coherence time (usually between two electronic states in the ground energy level) has garnered intense attention in the past decades.[3–18] In an optical dipole trap (ODT), the trapping potential experienced by the atom originates from the light-induced frequency shift (AC Stark shift) of its electronic states.[19] Different electronic states exhibit distinct energy shifts because of variations in their interacting parameters with the optical field. Therefore, the electronic state and the motional state of the atom are always bound together in an ODT.

Two primary decoherence mechanisms have been identified, and various schemes have been proposed to mitigate them. One decoherence mechanism is the variance of the differential energy shift (DES) between the two qubit states due to the noises associated with optical trapping and magnetic fields.[4,5] Many "magic trapping conditions", by which the variance of DES is immune to external noises, have been discovered to suppress the DES-related decoherence, such as magic polarization,[6,7] magic wavelength,[8–10,14] magic intensity,[3,11–14] and magic magnetic field.[8,9,13–16] The other mechanism of decoherence is due to the stochastically quantum jump between different phonon states, which is termed as the phonon-jumping-induced decoherence (PJID),[18] in which stochastic jumping of the atomic phonon state in an ODT can cause decoherence between the electronic states of the atoms. The variance of DES and the PJID can be suppressed by taking a blue-detuned ODT[20–26] and cooling the trapped single atom to its three-dimensional vibrational ground states.[18,27] The preceding works concerned the suppression of atom decoherence in optical traps with harmonic potential.

In this Letter, we study the dependence of the decoherence mechanism on the spatial form of the ODT. We found that a dipole trap with a higher-order spatial form possesses intrinsically low decoherence rates and therefore can provide a longer coherence time than the usually adopted harmonic trap.

2. Theory. To understand atomic decoherence in an ODT with an arbitrary spatial form, we first present a theoretical analysis. We consider a one-dimensional trap with spatial form $V(x) = \lambda x^{2l}$ (l is an integer), then the Hamiltonian of a particle in the trap is

$$H = \frac{p^2}{2M} + \lambda x^{2l}, \tag{1}$$

where p is the momentum, M is the mass of the particle. The wavefunctions and energies of the atom with Hamiltonian (1) are hard to solve directly with $l \neq 1$, but they can be obtained in the Hilbert space spanned by the eigenwavefunctions of any of a harmonic oscillator (HO). Especially, for a HO whose oscillation frequency ω fulfills the relation

$$\lambda = \frac{\hbar\omega}{4}\left(\frac{2M\omega}{\hbar}\right)^l, \tag{2}$$

*Corresponding authors. Email: gangli@sxu.edu.cn; tczhang@sxu.edu.cn
© 2025 Chinese Physical Society and IOP Publishing Ltd. All rights, including for text and data mining, AI training, and similar technologies, are reserved.

the Hamiltonian (1) can be reduced to

$$H = \frac{\hbar\omega}{4}(P^2 + X^{2l}), \tag{3}$$

where $P = \sqrt{\frac{2}{\hbar M\omega}}\, p$ and $X = \sqrt{\frac{2M\omega}{\hbar}}\, x$ are the dimensionless momentum and coordinate. The expressions of the wavefunctions and energies are the simplest. The analysis of the decoherence rates due to the variance of DES and the PJID can also be conducted conveniently.

For a real trap whose form is approximated by $V(x) = \lambda x^{2l}$, λ usually can be expressed as $\lambda = V_{\rm c}/a^{2l}$ with $V_{\rm c}$ the characteristic trap potential and a the characteristic size. According to Eq. (2) the trap frequency for the HO would be

$$\omega = \left(\frac{4V_{\rm c}}{\hbar}\right)^{\frac{1}{l+1}} \left(\frac{\hbar}{2Ma^2}\right)^{\frac{l}{l+1}}. \tag{4}$$

If a thermal atom with temperature T is considered, by following the procedures in Ref. [17] the variance DES between the two electronic ground states of the trapped atom can be expressed as

$$\mathrm{Var}(\Delta^{\rm DES}) = -\eta\frac{V_0}{\hbar}\frac{\mathrm{Var}(P_0)}{\bar{P}_0} + \frac{\eta}{(l+1)^2}\frac{k_{\rm B}T}{\hbar}\frac{\mathrm{Var}(P_0)}{\bar{P}_0}. \tag{5}$$

In this equation, $\eta = \omega_{\rm hfs}/\Delta_{\rm eff}$, where $\omega_{\rm hfs}$ and $\Delta_{\rm eff}$ are the hyperfine splitting and effective one-photon frequency detuning of the trapping laser, respectively. η is a factor that reflects the influence of hyperfine splitting between the two electronic states on the DES. V_0 is the trap potential at the position of the trapped atom. $\bar{P}_0$ is the average power of the trap light. $\mathrm{Var}(P_0)$ is the variance of the power. $k_{\rm B}$ is the Boltzmann constant. We have $k_{\rm B}T = \langle n\rangle\hbar\omega$ with $\langle n\rangle$ the corresponding mean phonon number of the HO. If V_0 can be set as zero, e.g., in a well-aligned blue-detuned trap, the second term will dominate $\mathrm{Var}(\Delta^{\rm DES})$. Atoms trapped with a potential with higher l will suffer a smaller decoherence due to the smaller $\mathrm{Var}(\Delta^{\rm DES})$ for a given relative power noise $\mathrm{Var}(P_0)/\bar{P}_0$.

For the decoherence caused by the PJID, we need to calculate the phonon jumping rate (PJR). The two heating sources, the heating due to the parametric noise and the beam-pointing fluctuation, can be dealt with separately in the perturbation theory.[28,29] The fractional fluctuations in λ and x are assumed to be $\epsilon_\lambda(t)$ and $\epsilon_x(t)$, respectively. The perturbations of interest are then

$$H'_\lambda = \epsilon_\lambda(t)\lambda x^{2l}, \tag{6}$$

and

$$H'_x = 2l\lambda x^{2l-1}\epsilon_x(t). \tag{7}$$

If the trapped atom is prepared in the phonon state $|n\rangle$ at time $t = 0$, the average rate that it transits to another state $|m \neq n\rangle$ due to the two perturbations is

$$R_\lambda = \frac{\pi\omega^2}{16}\sum_{m\neq n} S_\lambda(\omega_{mn})|\langle m|X^{2l}|n\rangle|^2 \tag{8}$$

and

$$R_x = \frac{\pi}{2\hbar}M\omega^3 l^2 \sum_{m\neq n} S_x(\omega_{mn})|\langle m|X^{2l-1}|n\rangle|^2, \tag{9}$$

respectively. Here, $S_\lambda(\omega)$ and $S_x(\omega)$ are the one-sided power spectrum of the fractional fluctuations in λ and x that are determined by the intensity noise and beam-pointing fluctuation of the optical trap light field; $\omega_{mn} = (E_m - E_n)/\hbar$ is the transition frequency between $|n\rangle$ and $|m\rangle$. $|\langle m|X^{2l-1}|n\rangle|^2$ and $|\langle m|X^{2l}|n\rangle|^2$ can be calculated in the Hilbert space spanned by the quantum states of the HO.

According to our previous work,[18] the overall coherence can be written as

$$\mathrm{C}(t) = \mathrm{e}^{-[\mathrm{Var}(\Delta^{\rm DES})]^2 t^2/2 - Rt}, \tag{10}$$

where $R = R_\lambda + R_x$ is the overall PJR. In a three-dimensional trap, the PJR in all dimensions needs to be summed over to give the overall R. From Eq. (5) we can see that $\mathrm{Var}(\Delta^{\rm DES})$ becomes smaller for larger l. In order to compare the PJR in ODTs with different spatial forms, we make the following assumptions: (1) the traps have the same characteristic potential $V_{\rm c}$ and size a; (2) the trapped atom is prepared in its ground phonon states; (3) the $S_\lambda(\omega)$ $[S_x(\omega)]$ stays the same for different traps. For a harmonic trap, we have $l = 1$, $\sum_{m\neq 0}|\langle m|X^{2l}|0\rangle|^2 = 2$, and $l^2\sum_{m\neq 0}|\langle m|X^{2l-1}|0\rangle|^2 = 1$. For a quartic trap, we have $l = 2$, $\sum_{m\neq 0}|\langle m|X^{2l}|0\rangle|^2 = 5.83$, and $l^2\sum_{m\neq 0}|\langle m|X^{2l-1}|0\rangle|^2 = 8.48$. Combined with Eqs. (8) and (9), we finally get $R_\lambda^{l=2} < R_\lambda^{l=1}$ under the condition $\omega^{l=2}/\omega^{l=1} < 0.59$ and $R_x^{l=2} < R_x^{l=1}$ under the condition $\omega^{l=2}/\omega^{l=1} < 0.49$. The smaller $\omega^{l=2}/\omega^{l=1}$ ratio, the lower the PJR in the quartic trap than in the harmonic counterpart. The situation in which the ODT has even higher-order spatial form can be analyzed in the same way.

3. Experiments. To verify the theory, we constructed two ODTs with harmonic and quartic spatial forms and compared the coherence times of the trapped atoms. We adopted Laguerre–Gaussian (LG) laser beams with a wavelength of $\lambda = 780\,\mathrm{nm}$ to build blue-detuned bottle trap (BBT) for trapping cesium (Cs) atoms. The experimental setup is similar to that of Ref. [30], and the schematic is demonstrated in Fig. 1(a). A collimated 780-nm Gaussian-mode laser beam is converted into a hollow LG beam (also known as a donut beam) by vortex phase plates. Vortex phase plates with topological charges $m = 1$ or 2 can create LG01 or LG02 mode beams.

A beam displacer is then used to split the donut beam into two spatially parallel beams separated by 4 mm. The polarizations of these two beams are orthogonal to each other. Then, a homemade NA = 0.4 objective with a focal length $f = 28.4\,\mathrm{mm}$ focuses these two donut beams. The two donut beams cross with each other in the focus at an angle $2\theta = 8^\circ$ and form a BBT.

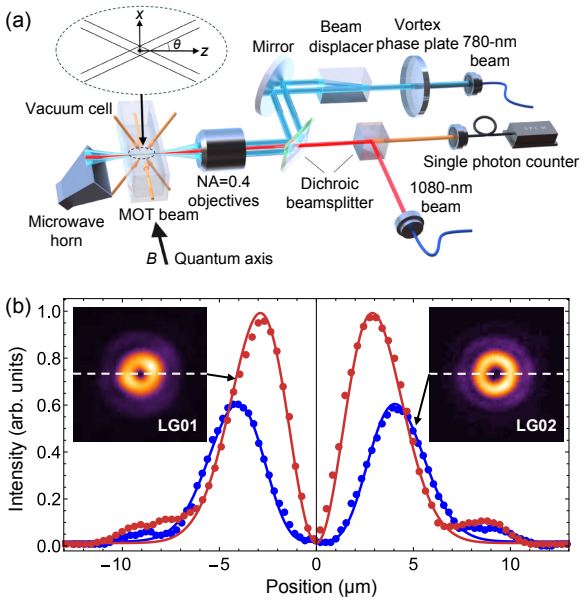

Fig. 1. (a) The experimental setup. A single Cs atom is captured by the 1080-nm red-detuned optical dipole trap (RODT) from magneto-optical trap (MOT) in the vacuum cell and adiabatically transferred into the 780-nm BBT. A microwave from the horn is used for coherent manipulation of the single atom. The atomic fluorescence is collected by the objective and detected using a single-photon detector. The sketch in the dashed circle shows the orientation of the two crossing donut beam at the focus of the objective. (b) The intensity distribution (solid dots) and the data fitting (solid lines) of LG01 and LG02 laser beams along the dashed lines in the inset images, which are the real images of LG01 and LG02 beams. The fitted waists of LG01 and LG02 beams are 4.09 and 4.05 μm, respectively.

To assess the mode quality of the LG beams, we captured images of these donut beams at equal power using a CCD camera. The insets in Fig. 1(b) show the images for the LG01 and LG02 beams, respectively. The intensity distribution across the center (shown as the dashed lines on the images) is extracted and fitted by the formula

$$I(r,z)=\frac{P(C_{lp}^{\mathrm{LG}})^2}{\pi w^2}\left[\frac{2r^2}{w(z)^2}\right]^{|l|}\mathrm{e}^{-\frac{2r^2}{w(z)^2}}\left[L_p^{|l|}\left(\frac{2r^2}{w(z)^2}\right)\right]^2, \quad (11)$$

where P is the total light power, $C_{lp}^{\mathrm{LG}}=\sqrt{\frac{2p!}{\pi(l+p)!}}$; $L_p^{|l|}$ is the Laguerre polynomial; l and p are the order of the orbital angular momentum and radial mode index ($p=0$, $l=1$ for LG01 mode and $p=0$, $l=2$ for LG02 mode); $w(z)=w_0\sqrt{1+(z/z_{\mathrm{R}})^2}$ with w_0 the waist and $z_{\mathrm{R}}=\pi w_0^2/\lambda$ the Rayleigh length of the LG beam. Figure 1(b) shows the data and the fitting curves. We can see that the intensity barrier of the LG01 beam is higher than that of the LG02 beam. The height ratio is 1.59, which is higher than the ideal value of 1.36 due to the larger diffraction of the LG02 phase plate. It is obvious that the spatial distribution around the core region of the beam is consistent with the theory.

The trap potential of the BBT formed by two LG01 and LG02 beams crossing to each other with angle 2θ [see Fig. 1(a)] can be expressed as $V(x,y,z)=-\frac{1}{2\epsilon_0 c}\alpha[I(x\cos\theta+z\sin\theta,y,-x\sin\theta+z\cos\theta)+I(x\cos\theta-z\sin\theta,y,x\sin\theta+z\cos\theta)]$ with ϵ_0, c, and α being the vacuum permittivity, the light speed, and the polarizability, respectively. The approximations of the BBT potentials to their lowest order around the trap center are [31]

$$V^{l=1}(x,y,z)\approx V_0\left(\frac{x^2}{a_{x,1}^2}+\frac{y^2}{a_{y,1}^2}+\frac{z^2}{a_{z,1}^2}\right) \quad (12)$$

and

$$V^{l=2}(x,y,z)\approx V_0\left(\frac{x^4}{a_{x,2}^4}+\frac{y^4}{a_{y,2}^4}+\frac{z^4}{a_{z,2}^4}\right), \quad (13)$$

respectively. Here, $V_0=-\frac{1}{2\epsilon_0 c}\alpha\frac{P}{\pi w_0^2}$ can be defined as the characteristic trap potential. The characteristic trap sizes are $\{a_{x,1},a_{y,1},a_{z,1}\}=\{w_0/(2\cos\theta),w_0/2,w_0/(2\sin\theta)\}$ and $\{a_{x,2},a_{y,2},a_{z,2}\}=\{w_0/(\sqrt{2}\cos\theta),w_0/\sqrt{2},w_0/(\sqrt{2}\sin\theta)\}$ for BBTs with LG01 and LG02 beams, respectively.

The comparison between the real trap potential and the lowest-order approximation is shown in Fig. 2. The characteristic sizes are exactly the coordinates of the trap bounds. Higher-order terms can be omitted in real experiments. Therefore, the theory of atom decoherence in different traps can be checked with these BBTs.

To efficiently load the single atoms into the BBT, an auxiliary 1080-nm red-detuned optical dipole trap (RODT) with a waist of 2 μm is employed to load a single cesium (Cs) atom from a cold Cs atomic ensemble. The center of the RODT is carefully aligned to overlap with the BBT. The fluorescence from the optically trapped single Cs atom, collected by the same objective, is sent to a single photon counter for detection. A 9.2-GHz microwave signal is applied by a microwave horn to coherently drive the Cs clock transition ($|F=4,m_{\mathrm{F}}=0\rangle\leftrightarrow|F=3,m_{\mathrm{F}}=0\rangle$). Here, we define the qubit as $|0\rangle\equiv|F=3,m_{\mathrm{F}}=0\rangle$ and $|1\rangle\equiv|F=4,m_{\mathrm{F}}=0\rangle$.

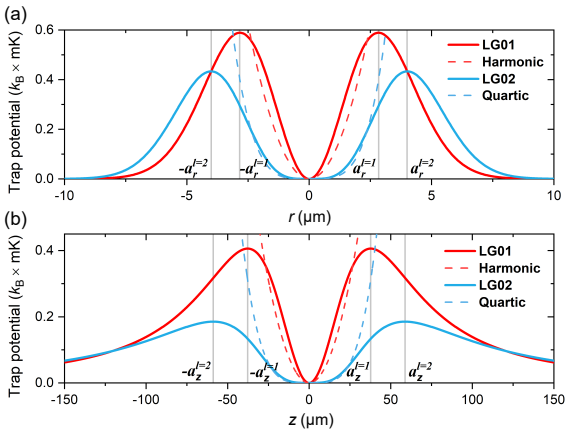

Fig. 2. The spatial dependence of the BBTs on (a) r and (b) z. Due to the small angle θ, the difference of the BBT spatial forms between x and y directions is tiny. Therefore, they are displayed by the same line with the horizontal coordinate r. The solid and dashed lines are the real potential distribution and the approximated harmonic trap. The red and blue lines represent the BBTs with LG01 and LG02 laser beams, respectively. The light gray vertical lines mark the bounds of the BBTs.

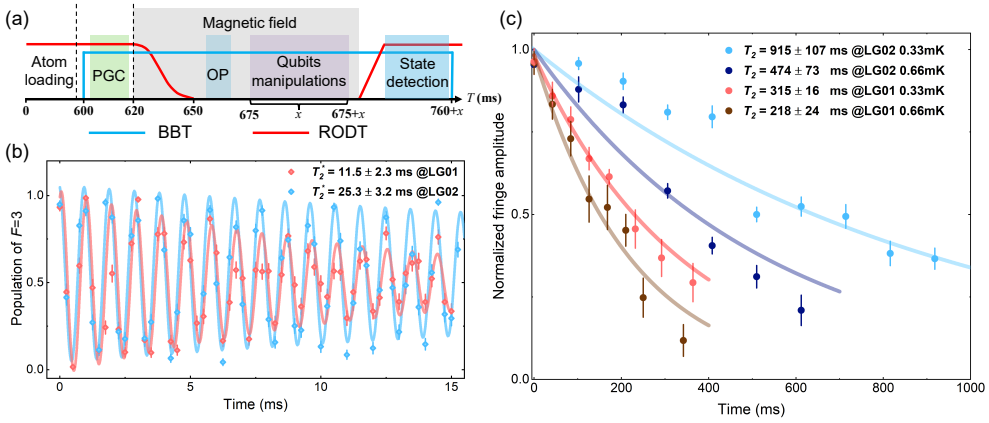

Fig. 3. Measurements of the coherence time. (a) The time sequence of the experiment. (b) The fringe of the Ramsey interferometer. (c) The decay of the coherence obtained by spin-echo under different trap settings.

The time sequence for the main part of the experiment is shown in Fig. 3(a), where the preparation phase for the cold atom ensemble via magneto-optical trap (MOT) is omitted. This sequence begins with the loading of single Cs atoms from the MOT by RODT with a time tag of 0 ms. The loading process lasts for 500 ms, during which the collisional blockade mechanism guarantees that a single Cs atom is loaded in the RODT. At 600 ms, the BBT is switched on and the single Cs is held by the combination of RODT and BBT for 20 ms. During this time, a 10-ms polarization gradient cooling is applied to cool the temperature to 10 μK. At 620 ms, the RODT is adiabatically switched off within 30 ms, leaving the BBT alone to hold the atom. It should be noted that the atom temperature drops to 5 μK after the adiabatic process. A 3-ms optical pumping (OP) phase is followed to prepare the atom in the $|F = 4, m_F = 0\rangle$ state. At 675 ms, the microwave pulses are applied to coherently manipulate the qubit. Finally, the RODT is switched on and the atom state is read by a state detection phase.

According to the theory of Refs. [5,17], a thermal atom trapped in an optical trap suffers mainly from inhomogeneous decoherence. The coherence time is mainly determined by the thermal temperature. The decoherence process can be measured using the standard Ramsey interferometer, in which two $\pi/2$-pulses are applied to the atom with a variable time delay in between. We studied this inhomogeneous decoherence process in both traps with the same trap potential at $V_0 = k_B \times 0.33$ mK. The results are shown in Fig. 3(b). The inhomogeneous coherence times T_2^* of the atoms in LG01 and LG02 BBTs are 11.5 ± 2.3 and 25.3 ± 3.2 ms, respectively. Inhomogeneous coherence times are almost the same, which means the same temperature. The dependence of T_2^* on atom temperature in a harmonic trap has been given in Ref. [5]. By analyzing the inhomogeneous decoherence in the Hilbert space associated with an oscillator whose oscillation frequency fulfills Eq. (2), the dependence of T_2^* on atom temperature in traps with spatial form $V(x) = \lambda x^{2l}$ should be fixed as

$$T_2^* = 0.97 \frac{(l+1)\hbar}{\eta k_B T}, \tag{14}$$

where k_B is the Boltzmann constant. A detailed derivation of Eq. (14) is provided in the Supplementary Materials (SM). Therefore, we can infer that the atom temperatures in LG01 and LG02 BBTs are 5.1 ± 1.0 μK and 3.5 ± 0.4 μK, respectively. A separate T_2^* measurements with LG01 and LG02 BBTs give results of 10.2 ± 1.0 and 11.6 ± 1.5 ms, and the corresponding temperatures are 5.8 ± 0.6 μK and 7.6 ± 1.0 μK, respectively. The average temperatures of the two measurements are 5.5 and 5.6 μK. They are consistent with each other and with those obtained from the release-and-recapture method, in which the temperature is determined by measuring the recapture probability of individual atoms after switching off the ODT for 10 μs intervals, followed by analysis using Monte Carlo simulations.

The inhomogeneous decoherence of the atom due to the thermal motion can be recovered by the dynamic decoupling techniques. Here, we adopted the simplest spin-echo process, in which a single π-pulse is inserted between two $\pi/2$-pulses, to recover the inhomogeneous decoherence. The residual decoherence is homogeneous and mainly determined by DES and PJID.[18] To compare homogeneous decoherence in the two types of traps, we measured the decay of coherence with time for atoms in traps with characteristic barrier heights of $V_0 = k_B \times 0.33$ mK and $V_0 = k_B \times 0.66$ mK, separately. The results are shown in Fig. 3(c).

We can see that the coherence time of a single atom in LG02 BBT is longer than that in LG01 BBT for the same V_0. However, because the characteristic trap sizes are different, direct comparisons are of little significance. Fortunately, if we decrease the characteristic trap potential of LG01 BBT from V_0 to $V_0/2$, equation (12) can be rewritten in the same form with new characteristic trap sizes $\{a_{x,1}, a_{y,1}, a_{z,1}\} = \{w_0/(\sqrt{2}\cos\theta), w_0/\sqrt{2}, w_0/(\sqrt{2}\sin\theta)\}$. This means that the LG01 BBT with characteristic trap potential $V_0/2$ and sizes $\{a_{x,1}, a_{y,1}, a_{z,1}\} = \{w_0/(2\cos\theta), w_0/2, w_0/(2\sin\theta)\}$ is equivalent to that with potential V_0 and sizes $\{a_{x,2}, a_{y,2}, a_{z,2}\} = \{w_0/(\sqrt{2}\cos\theta), w_0/\sqrt{2}, w_0/(\sqrt{2}\sin\theta)\}$. Thus, the comparison of atom coherence time in LG01 BBT with $V_0 = k_B \times 0.33$ mK to that in LG02 BBT with $V_0 = k_B \times 0.66$ mK makes more sense. From Eq. (4) we have $\omega^{l=2}/\omega^{l=1} = (\frac{\hbar^2}{8Ma^2V_0})^{\frac{1}{6}} = 0.074$. Combined with Eq. (5), we can conclude that the BBT with LG02 beams

has a lower decoherence rate than that with LG01 beams in theory. The experimental results of the coherence time 474 ± 73 ms in LG02 BBT versus 315 ± 16 ms in LG01 BBT solidly support the theoretical expectation. These results qualitatively verify our proposal that the ODT with a higher-order spatial form possesses a lower decoherence mechanism.

4. Conclusion. In conclusion, we proposed that the ODT with higher-order spatial form can provide an intrinsic lower decoherence rate than the counterpart with lower-order spatial form. We first formulated the atom decoherence rate by analyzing the variance of DES and the PJR, which are known as the two main decoherence mechanisms. Then, we experimentally proved our proposal by constructing blue-detuned harmonic and quartic traps with LG01 and LG02 laser beams and comparing the atom coherence time. Our method offers an alternative approach to enhancing atomic coherence time by modifying the spatial form of the ODT.

Acknowledgements. This work was supported by the National Key Research and Development Program of China (Grant No. 2021YFA1402002), the Innovation Program for Quantum Science and Technology (Grant No. 2023ZD0300400), and the National Natural Science Foundation of China (Grant Nos. U21A6006, U21A20433, 92465201, 12474360, and 92265108).

References

[1] Zhang X R, Zhuang X Y, and Liu X B 2025 *Chin. Phys. Lett.* **42** 047601
[2] Dai Y Q, Fu Y, Shi Z F, Qin X, Mu S W, Wu Y, Su J H, Deng Y F, Qin L, Zhai Y Q, Zheng Y Z, Rong X, and Du J F 2021 *Chin. Phys. Lett.* **38** 030303
[3] Guo R J, He X D, Sheng C, Wang K P, Xu P, Liu M, Wang J, Sun X H, Zeng Y, and Zhan M S 2024 *Chin. Phys. B* **33** 023701
[4] Kuhr S, Alt W, Schrader D, Dotsenko I, Miroshnychenko Y, Rosenfeld W, Khudaverdyan M, Gomer V, Rauschenbeutel A, and Meschede D 2003 *Phys. Rev. Lett.* **91** 213002
[5] Kuhr S, Alt W, Schrader D, Dotsenko I, Miroshnychenko Y, Rauschenbeutel A, and Meschede D 2005 *Phys. Rev. A* **72** 023406
[6] Choi J M and Cho D 2007 *J. Physics: Conf. Ser.* **80** 012037
[7] Kim H D, Han H S, and Cho D 2013 *Phys. Rev. Lett.* **111** 243004
[8] Derevianko A 2010 *Phys. Rev. Lett.* **105** 033002
[9] Derevianko A and Katori H 2011 *Rev. Mod. Phys.* **83** 331
[10] Kazakov G A and Schumm T 2015 *Phys. Rev. A* **91** 023404
[11] Yang J H, He X D, Guo R J, Xu P, Wang K P, Sheng C, Liu M, Wang J, Derevianko A, and Zhan M S 2016 *Phys. Rev. Lett.* **117** 123201
[12] Guo R J, He X D, Sheng C, Yang J H, Xu P, Wang K P, Zhong J Q, Liu M, Wang J, and Zhan M S 2020 *Phys. Rev. Lett.* **124** 153201
[13] Carr A W and Saffman M 2016 *Phys. Rev. Lett.* **117** 150801
[14] Li G, Tian Y L, Wu W, Li S K, Li X Y, Liu Y X, Zhang P F, and Zhang T C 2019 *Phys. Rev. Lett.* **123** 253602
[15] Sárkány L, Weiss P, Hattermann H, and Fortágh J 2014 *Phys. Rev. A* **90** 053416
[16] Chicireanu R, Nelson K D, Olmschenk S, Lundblad N, Derevianko A, and Porto J V 2011 *Phys. Rev. Lett.* **106** 063002
[17] Yang P F, Li G, Wang Z H, Zhang P F, and Zhang T C 2022 *New J. Phys.* **24** 083028
[18] Tian Z Z, Chang H B, Lv X, Yang M N, Wang Z H, Yang P F, Zhang P F, Li G, and Zhang T C 2024 *Optica* **11** 1391
[19] Li W F, Du J J, Wen R J, Li G, and Zhang T C 2015 *Chin. Phys. Lett.* **10** 104210
[20] Nie Y D, Sun Z G, and Fang Y R 2023 *Chin. Phys. B* **32** 018702
[21] Wang Z L and Yin J P 2005 *Chin. Phys. Lett.* **22** 1386
[22] Isenhower L, Williams W, Dally A, and Saffman M 2009 *Opt. Lett.* **34** 1159
[23] Xu P, He X D, Wang J, and Zhan M S 2010 *Opt. Lett.* **35** 2164
[24] Zhang P, Zhang Z, Prakash J, Huang S, Hernandez D, Salazar M, Christodoulides D N, and Chen Z G 2010 *Opt. Lett.* **36** 1491
[25] Barredo D, Lienhard V, Scholl P, de Léséleuc S, Boulier T, Browaeys A, and Lahaye T 2020 *Phys. Rev. Lett.* **124** 023201
[26] Almeida F, Sousa I, Kremer O, da Silva B P, Tasca D S, Khoury A Z, Temporão G, and Guerreiro T 2023 *Phys. Rev. Lett.* **131** 163601
[27] Wu T Y, Kumar A, Giraldo F, and Weiss D S 2019 *Nat. Phys.* **15** 538
[28] Savard T A, O'hara K M, and Thomas J E 1997 *Phys. Rev. A* **56** R1095
[29] Gehm M E, O'hara K M, Savard T A, and Thomas J E 1998 *Phys. Rev. A* **58** 3914
[30] Li G, Zhang S Y, Isenhower L, Maller K, and Saffman M 2012 *Opt. Lett.* **37** 851
[31] Zhang S Y, Robicheaux F, and Saffman M 2011 *Phys. Rev. A* **84** 043408